ƒ ‹ F | Œfia‹ ˙'e›ß• |–M^D‹ ª¤s›p e ƒ¤"G‡ł§i

ofii⁄@› ¥H† ¸›p⁄ "R‹ ´ƒ⁄§ƒ °⁄ ^ „¥ ¸¥H»†§U⁄ ¸ ßƒ ⁄ " · ¸⁄ flƒ""¶E´_

›p e^ § ¡G › §O«‹ ›p e
›p e‰ ¸s„¡GNSC94–2320–B–038–015–
ıƒ · ¶¡¡G94 ƒ~08 ⁄°01 ⁄ ø 95 ƒ~07 ⁄°31 ⁄Ø
ıƒ ‡ ƒ ¡G» O ¥´ ˙⁄j ˙´ ˙, ŒT‹ ª¤s'

›p e¥ D ø⁄¡HGfi } «•~
ƒ ¶P¥ D ø⁄¡HGfi}" a ¶ ' ¡ A "l⁄
›p e »P⁄H›ß¡G › S ‡flpA¶ ¥"N

‡ł§i^ «‹¡G" ° †‡ł§i
‡ł§i" ¥ ¡G¥ Xu Œ» • |˜‡‹ ª¤s⁄ –o‡ł§i⁄ ¸ o" ‰ ⁄
‡ B † zŁƒG¡¥»›p e¥ i ⁄ ‰ ¶‹ d,

⁄⁄ ¥` Œ 95 ƒ~10 ⁄°26 ⁄Ø

Abstract

This study investigates regional cerebral blood flow (rCBF) changes in patients with Parkinson's disease using independent component analysis (ICA) followed by statistical parametric mapping (SPM). **Methods:** ^{99m}Tc-hexaemethyl-propyleneamine oxime (^{99m}Tc-HMPAO) was used as the CBF tracer for rCBF measurements. A single photon emission computerized tomography (SPECT) study was performed on 62 patients with Parkinson's disease in various disease stages, and also on 51 aged-matched controls. SPECT images were first spatially normalized to standard space, concatenated, and then subjected to ICA decomposition. The resulting image components were then separated by logistic regression into two sets: disease-related components, whose subject weights differenced between groups and non-disease related components, whose subject weights exhibited no group difference. Components of each set were back-projected and summed across components. The resultant rCBF images were normalized to the global CBF for each subject and then analyzed using SPM to compare the rCBF values changes between Parkinson's disease and control subject. **Results:** In the disease-related image subspace, patients with Parkinson's disease exhibited significantly higher adjusted rCBF in the subthalamic nucleus, putamen, globus pallidum, thalamus, brainstem, and anterior lobe of cerebellum, and significant hypoperfusion in the supplementary motor plus dorsolateral prefrontal, pariteo-occipital cortex, insula, and cingulate gyrus. In the non-disease related image subspace, very few regions showed a significant group difference. Using SPM only without ICA separation gave significantly lower peak t value and at a smaller number of image voxels. Some of the regions revealed by ICA to be affected by Parkinson's disease have not shown significant changes in previous HMPAO-SPECT studies, though those are central to the pathophysiological model of Parkinson's disease. Finally, SVM could correctly classified normal controls from disease patient. **Conclusion:** In a HMPAO-SPECT study, ICA-based separation of normalized images into disease-related and unrelated subspaces revealed more disease-related brain regions than applying SPM directly. The diseased-related regions indicated by ICA are consistent with the current model of pathophysiology in Parkinson's disease, though their rCBF changes in Parkinson's disease have not been fully demonstrated by any previous single functional imaging study. Also, the SVM classification method could help clinical doctor diagnosis between PD and controls. Thus ICA combine with SVM method provides a new and

more comprehensive method for testing functional and brain circuit models in Parkinson's disease.
Key words: SPECT, Parkinson's disease, regional cerebral blood flow, Independent component analysis, statistical parametric mapping

中文摘要:
目前已有相當多的研究指出巴金森氏病人的腦血流與正常人有所不同，然而對於血流異常區域卻有許多不一致的發現，本研究試圖運用新的分析方法-獨立成份分析來分析巴金森氏病與正常人之單光子電腦斷層造影之不同。本研究收集 51 位正常人與 62 位不同程度之巴金森氏病人。腦血流測量使用 HMPAO 試劑，病人與正常人之腦影像，先使用標準化的模版做標準化。使每個影像的空間位置相同後，再把所有影像輸入做獨立成分分析，經由此分析後，以邏輯迴歸找出與疾病有相關之成分後，再以 SPM 的方法找出疾病箱關之腦血流異常區域，與過去的方法相比較，本研究不但發現傳統上在巴金森氏病典型的變化，包括基底核與小腦的腦血流增加，額葉與枕顳葉的腦血流下降，我們更發現輔助運動區與尾核的腦血流於病人有異常的下降，此發現能與疾病的病理生理學相符合。說明以此方法可以有效的發現疾病相關之異常腦血流區域，我們運用 Support Vector Machine (SVM)發展出巴金森氏症的輔助判別，並利用 Receiver Operator Characteristics (ROCs) curves 來作評估其效能。由獨立元件分析所得到的巴金森氏症大腦局腦血流異常區域當成特殊指標，運用 SVM 自動分類器依此指標來做資料的分類。研究結果顯示，運用此一完整的方式可以達到 ROC curves 下面積 98%，顯見這方法可以有效的協助臨床醫師做診斷上的協助指標。
關鍵詞：巴金森氏病、腦血流、獨立成分分析

Introduction

Parkinson's disease (PD) is a common neurodegenerative disease with four cardinal motor features: resting tremor, bradykinesia, cogwheel rigidity and postural instability. 99mTc-HMPAO SPECT is a well-established method of assessing rCBF. SPECT data have been analyzed utilizing either Region Of Interest (ROI) analysis (*4*), which investigates blood flow abnormalities in predefined regions, or using statistical parametric mapping (SPM), which can generate images of blood flow abnormalities for each pixel in the whole brain image(*5*). Results of previous reports about rCBF differences in PD and control have been mixed. Independent component analysis (ICA) is a recently developed data-driven approach to imaging data analysis. It has been widely applied to the analyses of functional neuroimaging data, including EEG/MEG, ERP, fMRI (*11*) and other biomedical signals. In the previous literature, ICA methods has been shown to effectively remove eye-blink artifacts in ERP study (*12*) and to

separate artifact components from fMRI data *(11)*. This study used ICA to remove the non-disease related SPECT activity including artifacts and rCBF unaffected by PD from the data followed by voxel-based statistic parametric mapping (SPM). We hypothesized that this method would reveal more areas of significant rCBF difference in PD.

Finally, most of neuroimage studies concerning disease-related pattern were focus on specific regions which came from their algorithm analysis. Few study really applied their specific regions to perform discrimination study between their disease and controls. Searching from PubMed web page by the keyword "discrimination, neuroimage and Parkinson's disease", only one study addressing this issue *(13)*. Compared with using neuroimage and Parkinson's disease as keyword to search in PubMed web, there are 26 studies focus on this topic. There is no study using SPECT or FDG-PET to perform study concerning differentiation of normal control from Parkinson's disease. The goal behind this study is to use one of machine classifiers, Support Vector Machine (SVM) to classified neuroimage comes from normal and Parkinson's disease. The automatic classification process will be evaluated in terms of receiver operator characteristics (ROCs) curves. This analysis allows us to evaluate the machine learning classifier in terms of their discrimination accuracy. These issues are important to the application of machine classifiers in PD research and to clinicians and researchers who would like to get an understanding of the classification process and analysis. Similar approaches may also be helpful in diagnosing other diseases.

MATERIALS AND METHODS

Subjects

Sixty-two PD patients and fifty-one age-matched control subjects participated in this study, included previously twenty-seven PD patients and twenty-four controls in the past study. Patients were diagnosed with PD according to the research diagnostic criteria of Ward and Gibb (*14*). Then stage of disease was assessed using the method of Hoehn and Yahr (*15*). The 62 PD patients (42 male, 20 female; mean age of 66.5+ 7 years) were divided into three groups; six patients at Hoehn-Yahr stage I, ten at stage II, and eleven at stage III. Patients were clinically evaluated using the motor-unified Parkinson's disease rating scale (UPDRS) prior to the SPECT study (*16*). Patients imaged had been maintained at least one month on stable anti-parkinsonian therapy with optimized clinical benefit. Patients were receiving anti-parkinsonian therapy including various combinations of L-DOPA with decarboxylase inhibitor (carbidopa), anticholinergic agents, amantadine hydrochloride and

dopamine receptor agonists. Fifty-one control subjects (15male, 36 female; mean age of 63.4 ± 6 years) were healthy volunteers without major neurologic or psychiatric disorder (including alcoholism, substance abuse, head trauma with consciousness loss or cerebral vascular disorder). All subjects were given information about the procedure and gave signed informed consent prior to participating in the study.

Experimental Protocol

Patients and control subjects were injected with 740MBq (20 mCi) of (99mTc) HMPAO 30 minutes prior to scanning. The acquisition matrix was 128x128; zoom, 1.5. The reconstruction of SPECT images was achieved using a filtered back projection algorithm with a Metz filter of power 3 and a system resolution of 8 mm intrinsic full width at half maximum (FWHM), resulting in 80 contiguous 128x128 transaxial image slices with in-plane resolution of 1.77x1.77 mm and slice thickness of 1.8 mm. Attenuation correction based on Chang's method (*17*) was performed on each slice, with a uniform attenuation coefficient of 0.11.

Image Transformation and ICA Pre-Processing

All images were first converted to Analyze format from their native image format using MRIcro software. Each individual SPECT image was then re-oriented and spatially normalized to the standard Montreal National Institute (MNI) template included in SPM2 http://www.fil.ion.ucl.ac.uk/spm/ using a 12-parameter affine transformation. As a result, each subject's image was re-sampled into 2x2x2 mm voxels in a cube with axes right-left, anterior-posterior, and superior-inferior, respectively. After spatial normalization, the individual SPECT images from normal controls (1~51) and patients (52~113) were concatenated, forming a SPECT data matrix, X, with 51 (the number of subjects) and 79*95*69 columns (the total number of voxels). ICA decomposition was performed under FMRLAB. Within FMRLAB, the off-brain voxels were first removed based on an image intensity threshold selected interactively through a graphic user interface. Then, the Bell-Sejnowski information-maximization (Informax) algorithm as implemented by Makeig et al. *(18)* was used to derive the spatially maximally independent components.

Independent Component Analysis

Applied to our SPECT data matrix, X, ICA found an 'unmixing' matrix, W, that decomposed or linearly unmixed the concatenated SPECT data into a sum of spatially independent components, $U = W \times X$, where U was a matrix of spatially fixed independent component SPECT images. Since the unmixing matrix W was invertible, $X = W^{-1} \times U$. The columns of W-1 represent relative signal strengths of the

component map in each of the observed subject SPECT maps X. That is, the signal amplitudes in the columns of W^{-1} represent the relative adjusted rCBF strength of the brain regions recruited by the corresponding component maps in each subject image. We expected that some of the resultant components would account for the differences in rCBF between (normal vs PD) groups, while other components would account for inter-subject variability in anatomy or rCBF. After ICA training converged, we applied logistic regression to the subject weights for each component, with a probability threshold of $p < 0.001$, to find "disease-related" components exhibiting a significant difference between patients (columns 52~113) and controls (columns 1~51). The remaining components were considered "non-disease-related" components. Thus, all the components were classified into two sets - "disease-related" or "non-disease-related". Components in these two sets were separately back-projected and summed to reconstruct the disease-related and un-related portions of the individual subject images.

Data analysis

SPM analysis was perform on both the raw SPECT images and on the reconstructed "disease-related" data pre-processed by ICA method described above. Before processing the raw data images, each image was spatial normalized using linear and non-linear parameters as in the ICA pre-processing step described above. Then a 3-D Gaussian filter (8 mm width) was used to smooth each image. The mean CBF of each image was scaled to 50 for each subject. Between-group comparisons (controls and PD), were performed on a voxel-by-voxel basis using as general linear model based on the theory of Gaussian fields (*19,20*), within SPM. The first comparison sought areas of increased perfusion, the second, areas of decreased perfusion. The resulting set of voxel values for each comparison constituted a statistical parametric map or SPM{t}. The SPM{t} maps were then transformed to unit normal distribution, SPM{z}. In these between-group comparisons, significant voxels were defined as those surviving a probability threshold of $p < 0.001$ after correction for multiple comparisons. In evaluating the data preprocessed by ICA, the two partial data sets (summing disease-related components and non-disease related components respectively) were submitted to SPM analysis separately as described above. SPM results on the raw and ICA preprocessed data were then overlaid on a normalized MR image.

Automatic classification base on SVM

SVM method was used to discriminate PD from controls base on the image

feature from previously result.

Results:

There was no significant difference in age between controls and patients. In the ICA-preprocessed data, 20 components were classified by logistic regression as “disease-related” and 93 components as “non-disease related”.

In whole image analysis by SPM, patients with Parkinson’s disease showed significantly increased adjusted rCBF in the putamen, globus pallidus, ventral lateral nucleus, brainstem, and cerebellum, while decreased adjusted rCBF was most prominent in the parieto-temporal and medial frontal cortex. Significant affects of Parkinson’s disease-related changes in ICA-preprocessed data were more extensive. In the “non-diseased related” component subspace, no area showed significance difference between groups. In contrast, in the “disease-related’ component set, Parkinson’s disease patients showed increased adjusted rCBF in the bilateral subthalamic nucleus, globus pallidus and putamen, ventral lateral and posterior nucleus of thalamus, brainstem, cerebellum, precentral gyrus, superior and inferior frontal cortex, as well as hypoperfusion in the bilateral middle frontal gyrus (dorsolateral prefrontal cortex), parieto-occipital cortex, temporal cortex, and cingulate gyrus. Details of the brain areas involved and a comparison of raw and Compared with the results from whole image data analysis, results on ICA- preprocessed data showed higher peak T values and more extensive regions of disease-related rCBF difference(figure 1).

In SVM classification, the sensitivity and specificity were 92% and 96% using SVM base on the image feature in PD in the dataset use in previously study. The area under receiver operator characteristics (ROCs) is 99% (figure 2). In this time, we also check the new dataset ROC and ROC from pool dataset (previously 51 cases and 62 cases). The ROC of new dataset was 0.98 and pool dataset was 0.99 (figure 2).

Discussion

Regions of rCBF increase in PD

Our data imply that in Parkinson’s disease, rCBF is increased in the basal ganglia, thalamus, orbital frontal cortex, the brainstem, and the cerebellum. Among these, increased rCBF in the bilateral putamen, globus pallidum, thalamus, subthalamic nucleus, and pons are expected from the basal ganglia circuit model (*2,3*) and are consistent with previous studies using SPECT and FDG-PET(*10,21*).

Regions of rCBF decrease in PD

A widely distributed decrease in rCBF in the cerebral cortex was found in PD from our result. The involved cortices included the posterior parieto-temporal cortex, precuneus,

cingulate, insula, dorsolateral prefrontal cortex, and supplementary motor cortex. In addition, the caudate and the medial dorsal nucleus of the thalamus also showed decreased rCBF.

The symptomatology in Parkinson's disease can be partially explained by a disturbed cortical-basal ganglia-thalamic-cortical circuit activity resuting from degeneration of dopaminergic nigrostriatal neurons. If such is the case, a consistent alteration of local rates of regional cerebral metabolism (rCMR) or regional cerebral blood flow (rCBF) would be expected. However, up to now, the findings of rCMR or rCBF changes in the brain of Parkinson's disease patients have been inconsistent. In this present study, we assess the rCBF changes between PD patients and normal controls using Independent Component Analysis as data preprocessing method. The rCBF changes in brain various brain areas shown in this study can well be incorporated into the suggested pathophysiological model in PD. In contrast to using SPM alone, the combination with ICA processing can reveal significant rCBF changes in areas that have been largely overlooked previously.

Conclusion

Our results show rCBF changes in PD are consistent with the current model of pathophysiology in PD. Using SVM separate PD from controls base on SPECT image's feature has good sensitivity and specificity. Although our sample data is not large, this method seems may be helpful in differentiating PD from health controls. Future application may be helpful in differentiating other Parkinson's plus syndrome. Further studies such as increase sample data or detail analysis of whole steps are needed to verify our methodology.

REFERENCES

[1] Hornykiewcz O. Dopamine (3-hydroxytyramine) and brain function. *Pharmacol Rev.* 1966;18:925-964.

[2] Albin RL, Young AB, Penney JB. The functional anatomy of basal ganglia disorders. *Trends Neurosci.* 1989;12:366-375.

[3] Alexander GE, Crutcher MD. Functional architecture of basal ganglia circuits: neural substrates of parallel processing. *Trends Neurosci.* 1990;13:266-271.

[4] Holman BL, Johnson KA, Gerada B, Carvalho PA, Satlin A. The scintigraphic appearance of Alzheimer's disease: a prospective study using technetium-99m-HMPAO SPECT. *J. Nucl. Med.* 1992;32:181–185.

[5] Imran, R. Kawashima S. Awata K. et al. Parametric mapping of cerebral blood flow deficits in Alzheimer's disease: a SPECT study using HMPAO and image standardization technique. *J. Nucl. Med.* 1999;40:244–249.

[6] Perlmutter JS, Raichle ME. Regional blood flow in hemiparkinsonism. *Neurology.* 1985;35:1127-34.

[7] Henriksen L, Boas J. Regional cerebral blood flow in

hemiparkinsonian patients: emission computerized tompgraphy of inhaled 133Xenon before and after levodopar. *Acta Neurol Scand*. 1985;71:257-266.

[8] Wolfson LI, Leenders KL, Brown LL, Jones T. Alterations of cerebral blood flow and oxygen metabolism in Parkinson's disease. *Neurology* 1985;35:1399-1405.

[9] Pizzolato G, Dam M, Borsato N, et al. (99mTc)-HMPAO SPECT in Parkinson's disease. *J Cereb Blood Flow Metab.* 1988;8(suppl):S101-S108.

[10] Imon Y, Matsuda H, Ogawa M, Kogure D, Sunohara N. SPECT image analysis using statistical parametric mapping in patients with Parkinson's disease. *J Nucl Med.* 1999;40;1583-89.

[11] McKeown MJ, Hansen LK, Sejnowsk TJ. Independent component analysis of functional MRI: what is signal and what is noise? *Curr Opin Neurobiol*. 2003;13:620-629

[12] Jung TP, Makeig S, Westerfield M, Townsend J, Courchesne E, Sejnowski TJ. Removal of eye activity artifacts from visual event-related potentials in normal and clinical subjects. *Clin Neurophysiol*. 2000;111:1745-58

[13] Eckert T, Sailer M, Kaufmann J, Schrader C, Peschel T, Bodammer N, Heinze HJ, Schoenfeld MA. Differentiation of idiopathic Parkinson's disease, multiple system atrophy, progressive supranuclear palsy, and healthy controls using magnetization transfer imaging. *Neuroimage. 2004* Jan;21(1):229-35.

[14] Ward CD, Gibb WR. Research Diagnostic Criteria for Parkinson's disease. In Streifler M, Korczyn AD, Melamed E, Youdim MBH (eds). *Advances in Neurology.* 1990;53,245-249.

[15] Hoehn MM, Yahr MD. Parkinsonism: onset, progression and mortality. *Neurology*. 1967;17:427-42.

[16] Fahn S. Elton RL, Members of the UPDRS Development Committee. Unified Parkinson's disease and movement disorders. In Recent Developments in Parkinson's disease vol2., Fahn S, Marsden CD, Calne DB, Goldstein M eds., Florham Park, NJ Mcmillan Health Care Information, pp. 153-164, 1987.

[17] Chang LT. A method for attenuation correction in radionuclide computed tomography. *IEEE Trans Nucl Sci.* 1978;25:638-43.

[18] Makeig S, Jung TP, Bell AJ, Ghahremani D, Sejnowski TJ. Blind separation of auditory event-related brain responses into independent components. *Proc Natl Acad Sci U S A*. 1997;94:10979-84.

[19] Friston KJ, Worsley KJ, Frackowiak RSJ, Mazziotta JC, Evans AC. Assessing the significance of focal activations using their spatial extent. *Hum Brain Mapping.* 1994;1:214-220.

[20] Friston KJ, Frith CD, Liddle PF, Frackowiak RSJ. Comparing functional (PET) images: the assessment of significant change. *J Cereb Blood Flow Metab*. 1991;11:690-699.

[21] Neirinckx RD, Canning LR, Piper IM Nowotnik DP, Pickett RD, Holmes RA, Volkert WA, Forster AM et al. Technetium-99m d.l-HM-PAO: a new radiopharmaceutical for SPECT imaging of regional cerebral blood perfusion. *J Nucl Med* 1987;28: 191-202.

[22] Payne JK, Trivedi MH, Devous MD Sr. Comparison of technetium-99mHMPAO and xenon-133 measurements of regional cerebral blood flow by

SPECT. *J Nucl Med* 1996;37: 1735-40.
[23] Kikuchi A, Takeda A, Kimpara T, et al. Hypoperfusion in the supplementary motor area, dorsolateral prefrontal cortex and insular cortex in Parkinson's disease. *J Neurol Sci.* 2001;193:29-36.
[24] Eidelberg D, Moeller, JR, Dhawan V, et al. The metabolic topography of Parkinsonism. *J Cereb. Blood flow Meta.* 1994;14:783-801.
[25] Lozza C, Marie RM, Baron JC. The metabolic substrates of bradykinesia and tremor in uncomplicated Parkinson's disease. *Neuroimage.* 2002;17:688-699.
[26] Dogali M, Fazzini E, Kolodny E, et al. Stereotactic ventral pallidotomy for Parkinson's disease. *Neurology*. 1995;45:753-761.
[27] Alvarez L, Macias R, Lopez G, et al. Bilateral subthalamotomy in Parkinson's disease: initial and long-term response. *Brain.* 2005;128:570-583.
[28] Antonini A, Vontobel P, Psylla M, et al. Complememtary positron emsission tomographic studies of the striatal dopaminergic system in Parkinson's disease. *Arch Neurol.* 1995;52:1183-90.
[29] Hilker R, Voges J, Weisenbach S, et al. Subthalamic nucleus stimulation restores glucose metabolism in associative and limbic cortices and in cerebellum: evidence from a FDG-PET study in advanced Parkinson's disease. *J Cereb Blood Flow Metab*. 2004;24:7-16.
[30] Mayberg HS, Starkstein SE, Sadzot B, et al. Selective hypometabolism in the inferior frontal lobe in depressed patients with Parkinson's disease. *Ann Neurol*. 1990;28:57-64.
[31] Berding G, Odin P, Brooks DJ, et al. Resting regional cerebral glucose metabolism in advanced Parkinson's disease studied in the off and on conditions with ((18)F)FDG-PET. *Mov Disord*. 2001;16:1014-1022.
[32] Black KJ, Hershey T, Hartlein JM, Carl JL, Perlmutter JS. Levodopa Challenge Neuroimaging of Levodopa-Related Mood Fluctuations in Parkinson's Disease. *Neuropsychopharmacology*. 2005;30:590-601.
[33] Firbank MJ, Colloby SJ, Burn DJ, McKeith IG, O'Brien JT. Regional cerebral blood flow in Parkinson's disease with and without dementia. *Neuroimage*. 2003;20:1309-1319.
[34] Antonini A, De Notaris R, Benti R, De Gaspari D, Pezzoli G. Perfusion ECD/SPECT in the characterization of cognitive deficits in Parkinson's disease. *Neurol Sci.* 2001;22:47-48.
[35] Arahata Y, Hirayama M, Ieda T, et al. Parieto-occipital glucose hypometabolism in Parkinson's disease with autonomic failure. *J Neurol Sci.*1999;163:119-126.
[36] Sestini S, Scotto di Luzio A, Ammannati F, et al. Changes in regional cerebral blood flow caused by deep-brain stimulation of the subthalamic nucleus in Parkinson's disease. *J Nucl Med.* 2002;43:725-732.
[37] Nagano-Saito A, Kato T, Arahata Y, et al. Cognitive- and motor-related regions in Parkinson's disease: FDOPA and FDG PET studies. *Neuroimage*. 2004;22:553-561.
[38] Ghaemi M, Raethjen J, Hilker R, et al. Monosymptomatic resting tremor and Parkinson's disease: A multitracer positron emission tomographic study. *Mov Disord* 2002;17:782-788.
[39] Porritt M, Stanic D, Finkelstein D, et al. Dopaminergic innervation of the human striatum in Parkinson's disease. *Mov Disord.* 2005 (published online)

計畫成果自評：

巴金森氏病是老年常見的神經退化性疾病，然而其缺乏有意義的生物學指標，使得診斷常需依靠臨床症狀診斷，如果能夠利用影像學的工具，找出與疾病相關連的異常區域，以此作為診斷參考指標，則能夠提高診斷的正確性，同時對於疾病的病理生理學將可提供更深入的了解，本研究發現以此方法，不但可以與過去的研究結果相符合，更可以找到過去研究無法發現，但從疾病的病理生理學可推論得知的異常區域，顯示以此新的方法更能有效的找到與疾病相關之異常區域。由獨立元件分析所得到的巴金森氏症大腦局腦血流異常區域當成特殊指標，運用 SVM 自動分類器依此指標來做資料的分類。研究結果顯示，運用此一完整的方式可以達到 ROC curves 下面積 98%，顯見這方法可以有效的協助臨床醫師做診斷上的協助指標。相關系統正改良設計中，以利下一年度的測試評估工作。

Figure 1. Regional CBF difference between PD and controls. (A). rCBF in controls higher than PD. (B) rCBF in PD higher than controls.

(A)

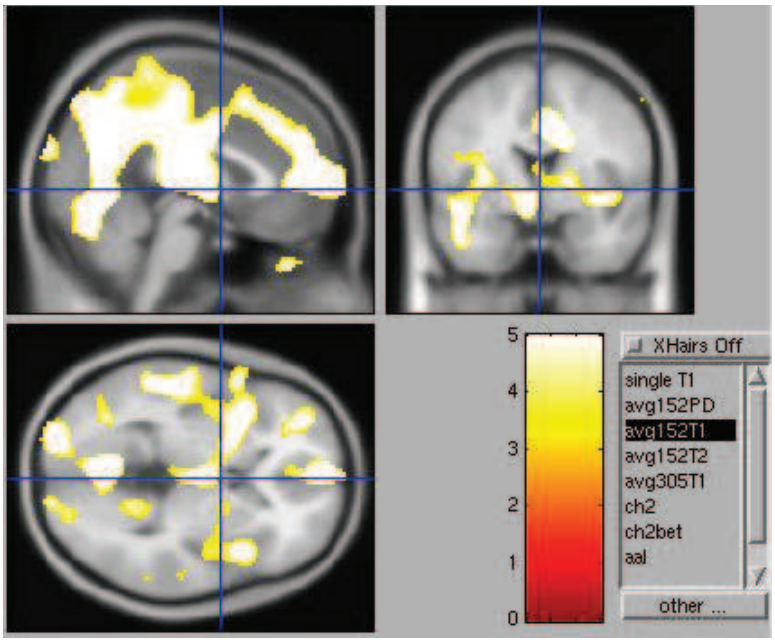

(B)

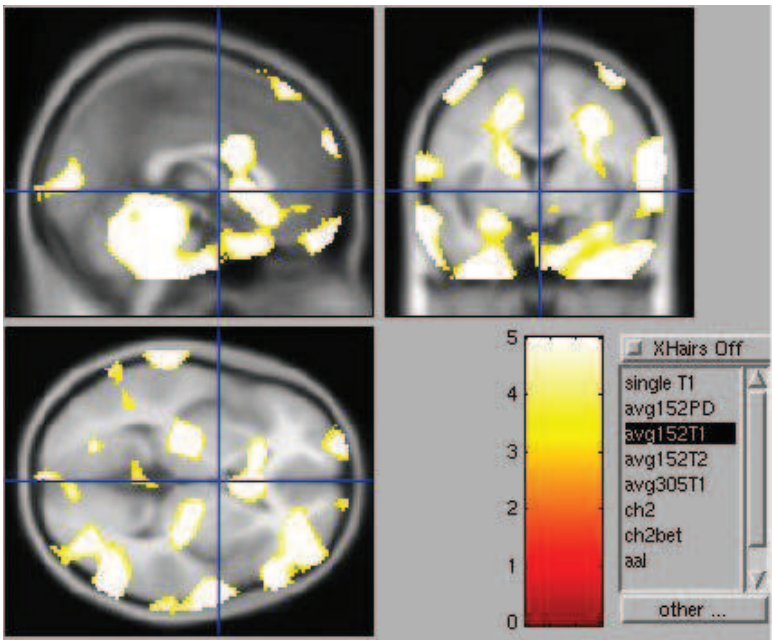

Figure 2. ROC by SVM method. (A) use previously 51 cases to make model and plot ROC figure. (B) new data use previous model to plot ROC figure.

(A)

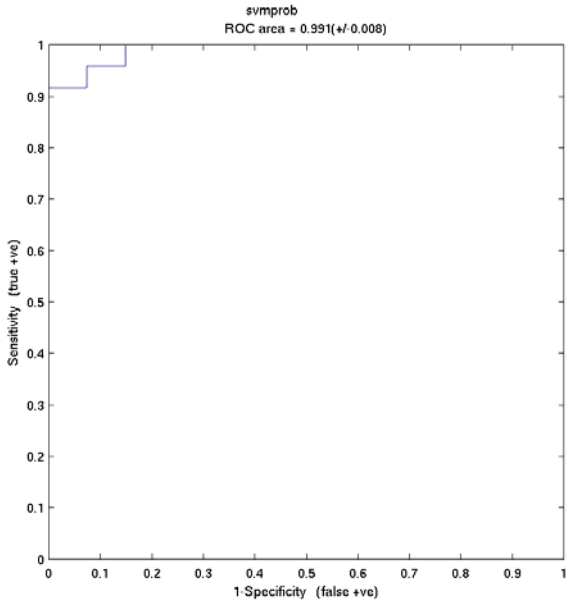

(B)

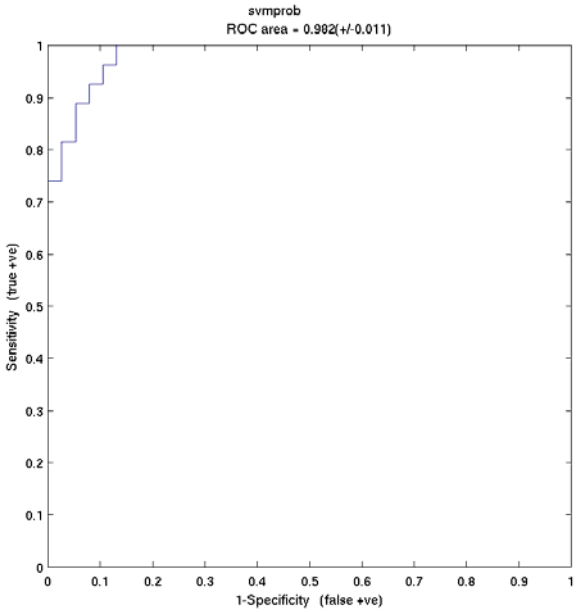
svmprob
ROC area = 0.982(+/-0.011)
Sensitivity (true +ve)
1-Specificity (false +ve)
0
0.1
0.2
0.3
0.4
0.5
0.6
0.7
0.8
0.9
1

附件二

可供推廣之研發成果資料表

☐ 可申請專利　☐ 可技術移轉　日期：95 年 10 月 30 日

國科會補助計畫	計畫名稱：發展一個以統計分析為基礎之自動分類器用以輔助及評估巴金森氏病的診斷 計畫主持人：徐建業 計畫編號：NSC 94 - 2320 - B - 038 - 015　學門領域：醫學工程
技術/創作名稱	輔助及評估巴金森氏病診斷之自動分類器
發明人/創作人	徐建業、徐榮隆、邱泓文
技術說明	中文：本研究試圖運用新的分析方法-獨立成份分析來分析巴金森氏病與正常人之單光子電腦斷層造影之不同。本研究收集 51 位正常人與 62 位不同程度之巴金森氏病人。發展一個以統計分析為基礎之自動分類器用以輔助及評估巴金森氏病的診斷。與過去的方法相比較，本研究不但發現傳統上在巴金森氏病典型的變化，包括基底核與小腦的腦血流增加，額葉與枕顳葉的腦血流下降，我們更發現輔助運動區與尾核的腦血流於病人有異常的下降，此發現能與疾病的病理生理學相符合。我們運用 Support Vector Machine (SVM) 發展出巴金森氏症的輔助判別，並利用 Receiver Operator Characteristics (ROCs) curves 來作評估其效能。由獨立元件分析所得到的巴金森氏症大腦局腦血流異常區域當成特殊指標，運用 SVM 自動分類器依此指標來做資料的分類。研究結果顯示，運用此一完整的方式可以達到 ROC curves 下面積 98%，顯見這方法可以有效的協助臨床醫師做診斷上的協助指標。
	英文：Independent component analysis (ICA) is a recently developed data-driven approach to imaging data analysis. This study investigates regional cerebral blood flow (rCBF) changes in patients with Parkinson's disease using independent component analysis (ICA) followed by statistical parametric mapping (SPM). the SVM classification method could help clinical doctor diagnosis between PD and controls. Thus ICA combine with SVM method provides a new and more comprehensive method for testing functional and brain circuit models in Parkinson's disease.
可利用之產業及可開發之產品	Medical Image, Image processing algorithms, Medical Decision support system

技術特點	目前已有相當多的研究指出巴金森氏病人的腦血流與正常人有所不同，然而對於血流異常區域卻有許多不一致的發現，本研究運用獨立成份分析來分析巴金森氏病與正常人之單光子電腦斷層造影之不同。腦血流測量使用 HMPAO 試劑，病人與正常人之腦影像，先使用標準化的模版做標準化。使每個影像的空間位置相同後，再把所有影像輸入做獨立成分分析，經由此分析後，以邏輯迴歸找出與疾病有相關之成分後，再以 SPM 的方法找出疾病箱關之腦血流異常區域。由獨立元件分析所得到的巴金森氏症大腦局腦血流異常區域當成特殊指標，運用 Support Vector Machine (SVM)自動分類器，依此指標來做資料的分類，達成巴金森氏症的輔助判別。研究結果顯示，運用此一完整的方式可以達到 ROC curves 下面積 98%，顯見這方法可以有效的協助臨床醫師做診斷上的協助指標。
推廣及運用的價值	如果能夠利用影像學的工具，找出巴金森氏病之神經退化相關連的異常區域，以此作為診斷參考指標，則能夠提高診斷的正確性，同時對於疾病的病理生理學將可提供更深入的了解。本研究成果可應用於醫學影像及醫學決策支援系統。